Biosensors and Bioelectronics 26 (2010) 404–410

Contents lists available at ScienceDirect

Biosensors and Bioelectronics

journal homepage: www.elsevier.com/locate/bios

Gold nanorod-based localized surface plasmon resonance biosensor for sensitive detection of hepatitis B virus in buffer, blood serum and plasma

Xiaohui Wang[a], Yuan Li[a], Huafen Wang[b], Qiuxia Fu[a], Jianchun Peng[a], Yingli Wang[a], Juan Du[a], Yong Zhou[a], Linsheng Zhan[a,*]

[a] Beijing Institute of Transfusion Medicine, Beijing 100850, PR China
[b] The 88th Hospital of PLA, Taian 271000, PR China

ARTICLE INFO

Article history:
Received 21 April 2010
Received in revised form 16 July 2010
Accepted 29 July 2010
Available online 4 August 2010

Keywords:
Biosensor
Gold nanorod
LSPR
Detection

ABSTRACT

A novel gold nanorods (GNRs) biosensor based on the localized surface plasmon resonance (LSPR) behavior was designed to detect the hepatitis B surface antigen (HBsAg) which indicates active viral replication of hepatitis B virus (HBV). The surface of GNRs was modified with monoclonal hepatitis B surface antibody (HBsAb) through physical adsorption. Raman spectrum, dynamic light scattering (DLS) and zeta potential measurement were conducted to access the nature of the GNRs after antibody modification. The binding of analyte to the molecular probe was monitored by the longitudinal wavelength shift of LSPR peak in the UV–Vis extinction spectrum resulting from the changes of local refractive index induced by the immunological reaction. The biosensor could be utilized in quantitative analysis in Tris buffers, which has dose-dependence response ranging from 0.01 IU/mL to 1 IU/mL. Further, the biosensor was suited for qualitative analysis of HBsAg in the actual media of blood serum and plasma. The ease of operation, high sensitivity, and its generality offer specific advantages over other GNRs-based immunoassay methods.

1. Introduction

Up to date, immunoassay plays a prominent role in the early diagnosis of cancer, infectious disease and autoimmune disorders. As the current gold standard, enzyme-linked immunosorbent assay (ELISA) has been one of the most extended methods for the serological diagnosis in protein detection in the last three decades. It still has some shortcomings, such as long testing time needed, indirect format of detection and multiple washing steps. In order to achieve rapid detection, gold colloid-based lateral-flow immunoassays have been extensively studied and utilized as field diagnosis and point-of-care technology. Efforts have been made to increase their detection limits, however, progress has been disappointing especially in quantitative analysis. Recently, with the development of nanotechnology, researchers are pushing the envelope to expand the applications of nanoparticles with unique properties to construct novel biosensors. For instance, quantum dots (Jain, 2004; Demidov, 2005; Shingyoji et al., 2005), carbon nanotubes (Ghosh et al., 2003; Wang et al., 2009), nanowires (Zheng et al., 2005) and magnetic nanoparticles (Baselt et al., 1998; Graham et al., 2002; Li et al., 2003; Millen et al., 2005; Li et al., 2006) have attracted much attention as signal transducers. However, the application of such biosensors are often limited by the solubility, stability, requirement for expensive instruments, and, most importantly, uncontrollable response to the compositions of complex biological samples. Generally speaking, practical sensors must work in the milieu of interest to minimize complexity of the system. Therefore, it is a big challenge for detection of varied samples in different matrices using the newly developed detection platforms. Since circumstances would have great influence on the behavior of biosensors, and there have been only a few reports (Osterfeld et al., 2008; Gaster et al., 2009; Xia et al., 2009) of novel immunoassays focusing on detecting protein in actual media, the aim of this study was to construct a method that would meet all these criteria and overcome the technological barrier to transfer bench research to clinical applications.

As is well known, gold nanorod (GNR) material has a larger light absorption and scattering cross section in the surface plasmon resonance wavelength regions (Hutter and Fendler, 2004; Pérez-Juste et al., 2005; Mayer et al., 2008; Anker et al., 2008) than gold nanoparticle (GNP) material (Chen et al., 2007). Unlike fluorophores, stable plasmonic nanoparticles do not blink or bleach, allowing researchers to observe molecular binding over arbitrary long time intervals. Anisotropic rod-shaped material gives rising to two absorption peaks corresponding to their plasmonic modes (Kelly et al., 2003; Pérez-Juste et al., 2005; Murphy et al., 2005). The longitudinal plasmon band has been demonstrated to be more sen-

* Corresponding author. Tel.: +86 10 66931292; fax: +86 10 66931292.
E-mail address: lszhan91@yahoo.com (L. Zhan).

0956-5663/$ – see front matter © 2010 Elsevier B.V. All rights reserved.
doi:10.1016/j.bios.2010.07.121

sitive than the transverse one observed for spherical particles both experimentally and theoretically (Pramod et al., 2007). As it has been demonstrated that the location of longitudinal plasmon wavelengths may reflect the changes in the dielectric properties of the surroundings and external environment, the nanosensor described in the present work is based upon the LSPR behavior of nanostructures that enables optical transduction of binding events into an optical signal. LSPR based biosensors can be conveniently modified by carbodiimide chemistry (Yu and Irudayaraj, 2007a,b). However, multiple modification steps resulted in difficulties in keeping the dispersion state from aggregation and made the monitoring of biospecific interactions events inaccurate. So in the present case, a feasible functionalization approach through nonspecific physisorption was designed. Crudely, an enveloped model of the GNRs was proposed and superior adaptability of such biosensors to external media was expected.

HBsAg is the most important marker for the laboratory diagnosis of hepatitis B. It in serum indicates an acute and chronic hepatitis B virus infection and potential infectivity. In this study, it has been taken as the example for the protein detection, namely, monoclonal HBsAb has been labelled on the surface of the GNRs through nonspecific adsorption to detect HBsAg. Some characterizations have been conducted to access the nature of the GNRs after biological modification. In addition, a validation experiment also has been designed in a 96-well microplate based on ELISA to evaluate the influence of steric effects on the binding affinity of the antibody–antigen pair. To our knowledge, it is the only report, that such homogeneous biosensor assay could work in the actual media to detect HBsAg in the presence of complex compositions in blood serum or plasma.

2. Materials and methods

2.1. Materials

All the reagents were used as received without further purification. Chloroauric acid and cetyltrimethylammonium bromide (CTAB) were purchased from Sigma–Aldrich Chemical Co. Sodium borohydride ($NaBH_4$), L-ascorbic acid and silver nitrate were purchased from Sinopharm Chemical Reagent Co. Ltd. Millli-Q purified water (18.2 MΩ) was used for all experiments. Bovine serum albumin (BSA) was purchased from Roche and monoclonal HBsAb was from Beijing Polaris Biotechnology Co, Ltd. The "Diagnostic Kit for Hepatitis B Surface Antigen" was provided by InTec Products, Inc. (Xiamen). HBsAg positive and negative serum samples used to evaluate the biosensor were obtained from the kit. The standard reference material for HBsAg was provided by the National Center of Clinical Laboratory (NCCL) of China.

2.2. Equipments for characterization

A Hitachi H-7650 transmission electron microscopy (TEM) operating at 80 kV was conducted to observe the morphology of the GNRs. Absorption spectra of GNRs and GNRs-based complexes at every stage were recorded with a SpectraMax M5 microtiter plate reader with Softmax® Pro Software (Molecular Devices Corporation, USA), with the wavelength ranging from 400 nm to 1000 nm. At least 120 μL of the sample was added to each well to obtain its absorption spectra. The charge and surface size of the nanoparticles and the complexes were measured by Zetasizer Nano ZS90 system (Malvern Instruments). Raman measurements were performed on a JY-HR800 Raman spectrometer. A He–Ne laser operating at $\lambda = 632.8$ nm was used as the excitation source. For each sample, 30 μL of the solution was dropped onto the glass slide and the spectrum was recorded after air drying. The isoelectric point (pI) of the proteins was determined by isoelectric focusing electrophoresis (PROTRAN IEF Cell, Bio-rad Corp. USA).

2.3. Preparation of GNRs

Gold nanorods were prepared using a seed-mediated surfactant-directed approach in a two-step procedure (Sau and Murphy, 2004). First, 250 μL 0.01 M $HAuCl_4$ aqueous solution was added to a solution of 7.5 mL 0.1 M CTAB, then the gold seed was generated by adding 600 μL 0.01 M freshly prepared ice-cold $NaBH_4$ solution to the CTAB solution in a test tube at once. The mixture was inversion mixed immediately for 2 min, followed by being kept in a water bath at 25 °C for at least 2 h. And the next was to prepare the nanorod growth solution, which was prepared by adding the several reagents to 95 mL 100 mM CTAB with gently shaking in the following order: 4 mL 10 mM hydrogen tetrachloroaurate (III), 600 μL 10 mM silver nitrate and 640 μL 100 mM ascorbic acid. Then, 100 μL of this seed solution was added to the growth solution prepared before, mixed for 10 s by shaking and left undisturbed for 3 h before washing. Excess CTAB was removed from the GNRs suspension by centrifugation at 8000 rpm for 10 min. The GNRs were redispersed in deionized water, which was concentrated to c.a. 0.5 nM by sonication and centrifugation before use.

2.4. Biological modification of as-prepared GNRs

In this work, the as-prepared GNRs were directly modified by monoclonal HBsAb through physical adsorption. Briefly, 200 μL of concentrated GNRs was added to 1.0 ml 0.1 mg/mL HBsAb aqueous solution at room temperature with gentle shaking, followed by being kept still for 30 min. Then, the antibody-labelled GNRs were washed by 1 wt.% BSA solution (10,000 rpm, 10 min for purification) and centrifuged three times.

2.5. Validation experiment based on ELISA

In validation experiment, all the reagents and steps were the same as which being employed in the sandwich ELISA, except that monoclonal HBsAb-labelled GNRs were used instead of monoclonal HBsAb attaching to the surface of a 96-well microplate. Simultaneously, a routine ELISA procedure was performed on the same microplate for comparison. The amount of HBsAb in GNRs-HBsAb was determined by a BCA™ Protein Assay Kit (Pierce).

2.6. In vitro diagnosis with the fabricated biosensor

In the detection stage, the working reagent was prepared by adding the functionalized GNRs to 10 mM Tris buffer before the unknown samples added. Study of optimization conditions provided the proper working concentration for GNRs, which could be controlled by rescaling the maximum absorbance of the longitudinal plasmon peak in the detection system. An hour of incubation was performed to allow the probe-target binding to reach equilibrium. Products of the immunological reaction were collected by centrifugation and resuspension, and then absorption spectra were measured between 400 nm and 1000 nm and peak shifts were recorded. Each peak shift value was averaged from three parallel experiments and expressed as mean ± standard deviation.

3. Results and discussion

3.1. Characterization of GNRs and the fabricated biosensor

Fig. 1 is the schematic representation of the synthesis of monoclonal HBsAb conjugated GNRs and the detection mechanism for

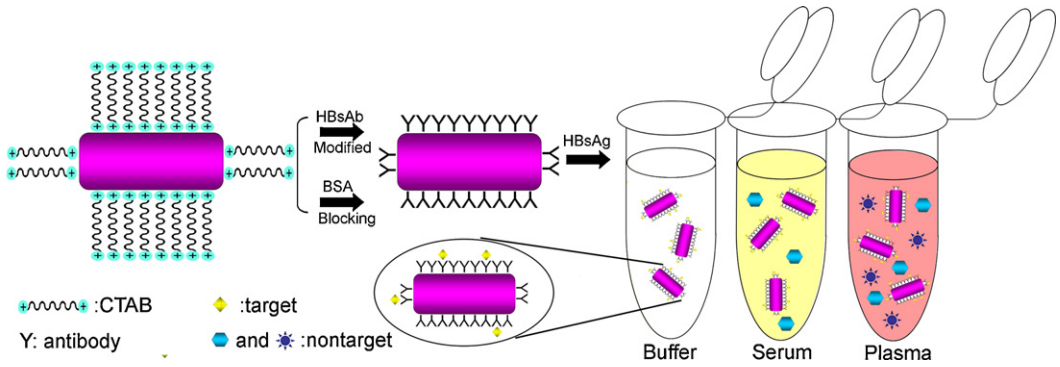

Fig. 1. Schematic representation of the synthesis of antibody-functionalized GNRs and the detection mechanism for the biosensor immunoassay in capturing targets in different matrixes.

such biosensor in capturing targets. In the current work, antibody functionalization is simply done by incubating antibody with concentrated GNRs through nonspecific physisorption. Actually, the majority of the modifications of GNRs were through EDC/NHS reagents, in which at least two steps were needed to implement the process. This is because chemical modification was desirable to obtain a more sensitive biosensor based on the terminal modification model (Yu and Irudayaraj, 2007a). However, other direct evidence for this model was absent except for some studies concerning the oriented assembly phenomenon (Caswell et al., 2003; Chang et al., 2005; Huang et al., 2010). On the other hand, the homogeneous immunoassay for cancer biomarker detection with GNRs and GNPs modified through physical adsorption coupled with dynamic light scattering (DLS) has been established with a dose-dependent result (Liu et al., 2008). In view of the above facts, we adopted the physical adsorption modification to simplify the fabricating process.

After incubating with HBsAb and washing by BSA, the active sites remaining after antibody adsorption were considered completely blocked. The obtained complex is the so-called biosensor, which can distinguish target proteins. When the homogenous system reaches equilibrium, the biosensor's response to target binding can be monitored by the red shift of transverse and longitudinal electronic oscillation, in which the latter is more sensitive, as has been demonstrated by this work and in agreement with many groups (Yu et al., 2007; Pramod et al., 2007; Wang and Irudayaraj, 2008; Huang et al., 2009). The pronounced red shift of the nanoparticle and antibody–antigen complex results from the changes of the effective thickness of the adsorbate layer, the refractive index of the adsorbate and medium surrounding and electromagnetic field decay length, while the chosen nanomaterial determines the sensitivity factor (Chen et al., 2007; Anker et al., 2008). The longitudinal plasmon band of the GNRs which had been chosen to use in this work is located at c.a. 700 nm, because in this wavelength range the background absorption, scattering, polarization and spectral characteristics of endogenous chromophores from biological mixtures (for instance, hemoglobin in serum and blood) was minimal (Weissleder, 2001).

Fig. 2 shows a typical TEM micrograph (A) of the as-prepared GNRs, characteristic plasmon absorption spectrum (B) and Raman spectra (C) for the GNR material before and after HBsAb functionalization. Fig. 2(A) shows fairly uniform rod-shaped nanoparticles (a length of 68 ± 8 nm and a width of 30 ± 5 nm) with a high yield has been synthesized. The inset micrograph exhibits a good dispersion of the GNRs at a certain concentration. As shown in Fig. 2(B), after HBsAb modification, the red shift related to the longitudinal plasmon band of c.a. 10 nm occurs. It should be assigned to the changes of the thickness of the adsorbate layers and their refractive indexes. Comparison of the LSPR spectra of GNRs and GNRs-HBsAb indicates that the ratio of the transverse LSPR peak to the longitude LSPR peak keeps constant. However, increase of this ratio has been observed after GNRs functionalized in other researches (Marinakos et al., 2007; Yu et al., 2007), which was related to the formation of an end-on configuration. Here, the constant ratio suggests the primary dispersion state of the GNRs was maintained after antibody modification. Further, after incubation with HBsAg, a pronounced red shift of the longitudinal band can be observed as a plasmon response of the fabricated biosensor to the target, which could be due to the binding events that resulted from the immunological reaction. It should be noticed that the capturing of HBsAg has led to a larger magnitude of shift for the LSPR peak in comparison with that in binding of HBsAb. In addition little difference of the shape and half-width of the spectrum presents after capturing the target, suggesting a controllable dispersion state of the nanoparticles from aggregation.

Raman spectrum reading of pure CTAB, GNRs before and after antibody functionalized have been recorded and presented in Fig. 2(C). The spectra for GNRs and GNRs-HBsAb have more intense spectral signals than pure chemicals, probably due to the surface-enhanced Raman scattering effect in the presence of GNRs. Therefore, for comparison purpose, all spectra have been normalized. The spectra for pure chemical CTAB matches well with those spectra given in other studies (http://riodb01.ibase.aist.go.jp/sdbs/cgi-bin/direct_frame_top.cgi, Foucault et al., 2003). As shown, before modification, the CTAB-capped GNRs, display characteristic CTAB Raman bands at 763 cm^{-1} and 1460 cm^{-1} (http://riodb01.ibase.aist.go.jp/sdbs/cgi-bin/direct_frame_top.cgi; Kalyanasundaram and Thomas, 1976; Foucault et al., 2003; Yu et al., 2007), which accords with the spectrum of CTAB below. In the case of GNRs-HBsAb, the poor signal-to-noise ratio brings about difficulties in differentiating peaks from the background noise. However, it is worth noting that the peaks associated with CTAB have disappeared, with some new peaks arising. Among them, the 851 cm^{-1} peak can possibly be assigned to the tyrosine ring breathing vibration (Huang et al., 2007), and the 1003 cm^{-1} to ring C–C stretch vibrations in the phenylalanine residues (Huang et al., 2007), demonstrating that the antibody molecules were adsorbed on the surface of the GNRs. This suggests that at least the majority of the CTAB molecules had been replaced by adsorbed protein molecules in modification. While in the detection step, HBsAg molecules bond to the GNRs probe through immunological reaction. In other words, such replacement did not occur to reduce the changes of the effective thickness of the adsorbate layer. This is maybe the reason why the LSPR shift in detection was much larger than that in the modification step.

Additionally, zeta potential analysis and DLS measurement were used to further confirm the surface modification by antibody. Zeta potential analysis gave +27 mV and −32 mV for GNRs before and after antibody modification, respectively. The isoelectric point of

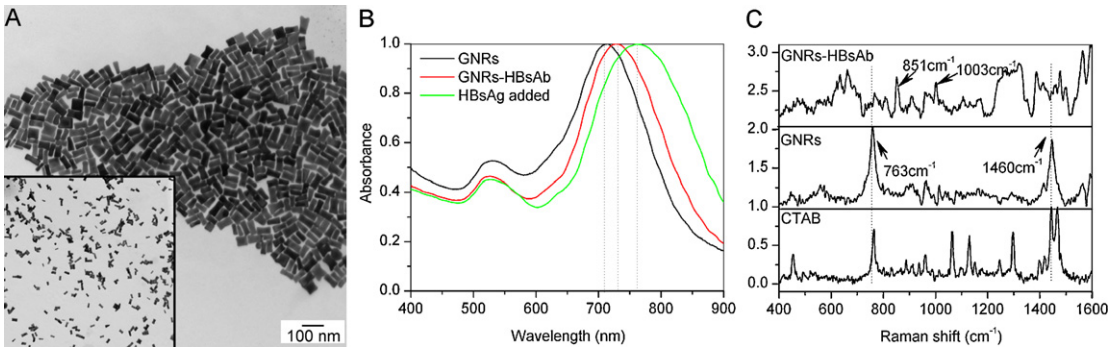

Fig. 2. Typical TEM micrographs (A) of the as-prepared GNRs, characteristic plasmon absorption spectra (B) and Raman spectra (C) for the GNR material before and after HBsAb protein functionalization. The inset micrograph in (A) exhibits a good dispersion of the GNRs at a certain concentration.

the monoclonal HBsAb has been determined by isoelectric focusing electrophoresis to be 6.2. The pH value of the modification system was measured to be 5.6, higher than the pI value of HBsAb. Since the HBsAb molecules in this system also had positive charges, it can be concluded that nonspecific physisorption has occurred between GNRs and HBsAb molecules during the modification step. In the case of BSA, because the pI value for it was 4.7, it was negative charged in this system. Thus, the remaining sites where CTAB still being should have been blocked by BSA through electrostatic interaction. As a result, after modification, the net charge for the functionalized GNRs was negative, consistent with the zeta potential analysis. DLS was utilized to monitor the size changes of the nanoparticles. Before modification, the Z-average diameter of the GNRs was measured as 62.1 nm, while after antibody functionalized, it was increased to 89.7 nm. It can be noted that the size of nanorods according to DLS is much larger than the data described above from TEM micrographs, which may be attributed to two points as follows. One is the CTAB surfactant layer adsorbed on the surface of the GNRs, and the hydrodynamic radius is obtained by DLS, which is the effective size of the particle as detected by its diffusion, a layer formed by its counterions involved. The other, which is more important, is that the size by DLS is weighting of light scattering intensity, not number weighting as it is in TEM. The difference in the calculation principle makes the results of DLS larger. Since the CTAB layer is a bi-layer with a thickness of 4–5 nm and the antibody molecules have a size of 6–10 nm, the size increase is readily interpreted.

3.2. Validation experiment

In this work, we utilize gold nanorods as an optical transducer and the wavelength shift of the longitudinal electronic oscillation is recorded as the optical signature of biosensor-analyte capturing events. However, would being labelled by nanoparticles affect the binding affinity between antibody and antigen or not? This is the key factor which might have great influence on the limit of detection and specificity of the fabricated biosensor. To resolve this problem, a validation experiment was designed in a 96-well microplate based on ELISA, as illuminated in Fig. 3.

Moreover, as is well known, standard materials are often stable in their own properties. To make all the results obtained in this work comparable with other studies and minimize the effect of binding affinity resulting from different antigen/antibody pairs, HBsAg standard material was applied to play the role of analyte in this work.

No matter in the case of Fig. 3(A) or (B), the concentration of monoclonal HBsAb, polyclonal HBsAb and enzyme labelled antibody remain equal in each well. Furthermore, for comparison purpose, the effective amount of HBsAb in GNRs-HBsAb of group B is equal to that of group A in alkaline diluted solution. As have been depicted in Fig. 1, after functionalized, the nanorod was surrounded by the monoclonal HBsAb molecules. In the coating step of ELISA, no matter through which side the GNRs contacts with the microplate, half of the monoclonal HBsAb molecules can be considered as effective ones. The concentration of effective HBsAb can be determined by the optimized conditions according to the conventional ELISA using the same antigen/antibody pair. A blank experiment was carried out to evaluate the color interference brought about by GNRs, which demonstrated it contributed negligibly to the final results.

The *t*-test was adopted to compare the actual difference between the data of the two groups. And it is interesting to observe that there was no statistical significance between groups A and B, as shown in Fig. 3 (C) and (D), which corresponding to the coating model of groups A and B, respectively. Besides, the limits of detection (LOD) of them remain equal to each other to be 0.4 IU/mL. Similar results have been obtained by Hafner's group (Mayer et al., 2008). In their study, after the gold nanorods were fixed to a glass surface and conjugated to antibody by carbodiimide cross-linking, the binding rates and equilibrium constant could still keep in good agreement with literature values for an antibody–antigen system. Combined with our results, it can be concluded that the steric effect is not dominant after antibody conjugates with gold nanorods, which gives us a large development space to increase the sensitivity of such biosensors.

3.3. Quantitative analysis of HBsAg in aqueous solution

Fig. 4 is a plot of the longitudinal LSPR shift over the target HBsAg concentrations ranging from 0.01 IU/mL to 1 IU/mL. It is obvious that a sigmoidal correlation exists over this range according to standard material. Our experiment indicates that gold nanorod-based LSPR biosensor is capable of measuring HBsAg concentration even at 0.01 IU/mL level, which is about 40 times lower than the LOD of the ELISA method under the optimized conditions. By using the GNRs-based biosensor assay, similar sigmoidal dose–response curve also has been plotted in the literatures (Marinakos et al., 2007; Nusz et al., 2009). It is worth noting that the red shift of the assay would not increase linearly with the protein concentration increased, because the theoretical maximal combining amount of the target protein is easily calculated by the above experimental data according to the previous literature (Yu et al., 2007) and is estimated to be between 20 IU/mL and 200 IU/mL. However, the actual value will be much less than the theoretical value because the standard 1:1 binding model was applied in estimation.

3.4. Qualitative analysis of HBsAg in blood serum and plasma

Great efforts have been made to develop a general sensing platform that can be ubiquitously applied to detect the constellations of biomolecules with high sensitivity and specificity in diverse clinical

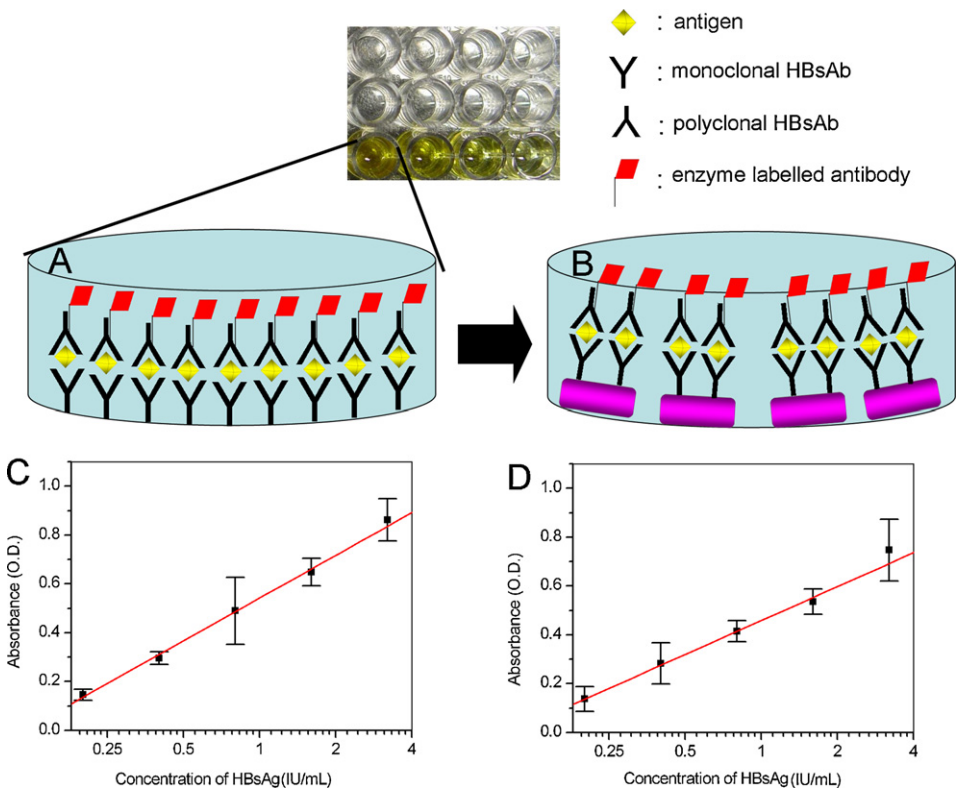

Fig. 3. Schematic illustration of the validation experiment designed in a 96-well microplate based on ELISA. It has been demonstrated that the steric effect is not dominant after the antibody conjugated with the gold nanorods.

samples, such as blood serum, plasma, urine, cell lysate and so on. To the best of our knowledge, little work (Marinakos et al., 2007) has been done in applying GNRs-based SPR or LSPR biosensors to capture a target in more complex media than water or buffer. The major limitation is the signal distortion that is caused by nonspecific adsorption of other proteins in the medium besides targets. Generally speaking, chemical modification is always preferred employing in fabricating such biosensors. The most likely reason for the nonspecificity might be that some active sites still remain on the GNRs after chemical modification, for the surface CTAB molecules could hardly be completely displaced by chemical reactions under mild conditions (Wang and Irudayaraj, 2009). However, our GNR-based biosensor was fabricated by physical adsorption with corresponding antibody, especially sufficient BSA blocking followed by it. This treatment made the biosensor a flexible shell composed of protein molecules, which would permit such sensors to work in other media of interest without unnecessary changes of solution to minimize complexity.

Therefore, HBsAg positive and negative serum samples were first applied to evaluate our biosensor. To obtain more information about the assay, blank and control (BSA added) samples were also tested in the same run. The results after normalization were displayed in Fig. 5. As shown, no obvious difference between the spectra of blank and control was observed. By contrast, comparing with the negative serum sample, the positive serum showed an 8 nm red shift. In practice, 6–20 nm red shifts were obtained according to different batches of the diagnostic kits.

For bedside diagnosis, blood plasma serves as an analyte that can rapidly be prepared by spinning a tube of fresh blood in a centrifuge until the blood cells are suspended. It is mostly water (90% by volume) and contains dissolved proteins, glucose, clotting factors, mineral ions, hormones and carbon dioxide. In the current study, we next aimed to demonstrate the usefulness of our assay system for detecting HBsAg in blood plasma. Twenty-three clinical plasma samples that had been previously identified by ELISA as positive or negative were analyzed with the fabricated biosensor. To increase the level of confidence, a control experiment was carried out. In the control experiment, 50 ng/mL of the BSA solution was added to the homogeneous detection system in parallel with clinical plasma samples. The maximal average shift of the control experiment was 1.7 nm (blue or red) compared with the blank experiment. In practice, the peak locations of control and blank experiment always match well with each other. For the majority, less than 1 nm shift was observed, indicating the complete blocking could decrease the nonspecific signal of our LSPR-based biosensor.

From the experimental data listed in Table 1, it can be noted that 12 positive samples all have red shifts, ranging from 4.3 nm to 30 nm relative to blank experiment. Meanwhile, less than ±3 nm shift occurred for the negative samples compared to the blank,

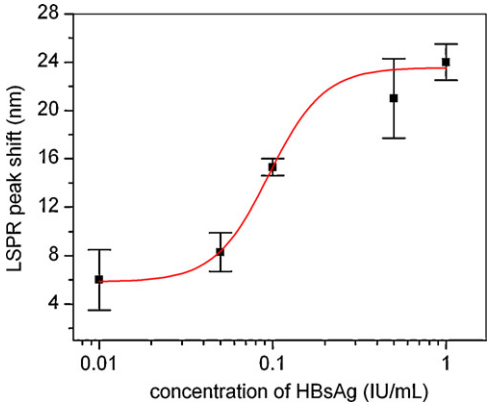

Fig. 4. A plot of the longitudinal LSPR shifts over the target HBsAg concentrations ranging from 0.01 IU/mL to 1 IU/mL. A sigmoidal fitting curve exists in the range.

Table 1
The longitudinal LSPR shifts of the fabricated biosensor in capturing HBsAg in clinical plasma samples, the results of which accord well with a routine ELISA.

Sample number	Positive samples (nm)	Negative samples (nm)	Sample number	Positive samples (nm)	Negative samples (nm)
1	7.3 ± 3.0	2.7 ± 1.6	7	11.3 ± 1.9	1.4 ± 2.9
2	18.8 ± 2.5	0 ± 1.3	8	17 ± 0.8	1.1 ± 1.7
3	16.3 ± 3.7	−0.6 ± 0.8	9	7.3 ± 2.6	0.7 ± 1.3
4	11.7 ± 2.6	−0.3 ± 0.4	10	12.3 ± 5.7	0.4 ± 1.4
5	4.4 ± 0.4	1 ± 0.9	11	30 ± 5.3	−1 ± 0.5
6	16.3 ± 3.1	1.4 ± 2.2	12	26.3 ± 5.2	/

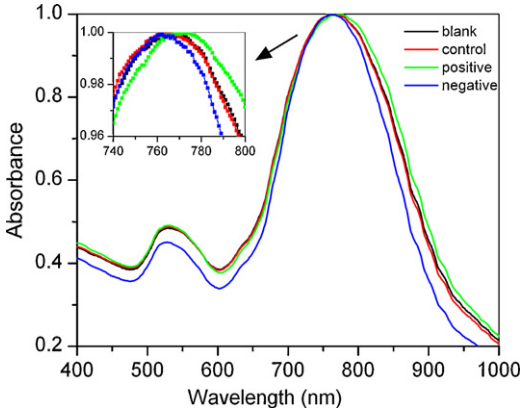

Fig. 5. The biosensor's behavior in qualitative analysis of positive and negative serum. From the magnified graph indicated by the arrow, a difference can be easily observed between the positive and negative serum.

which could be attributed to the noise of the assay. Most of the antibodies are negatively charged under the physiological pH, while GNRs-based biosensors are also negative charged according to the zeta potential results, which minimizes physical adsorption due to electrostatic repulsion to yield better blank and control. Combined with the results of the control experiments, it can be concluded that the fabricated biosensor has a good specificity which could not be disturbed by other proteins or components in plasma. Thus, as expected, coincident results were achieved by this biosensor assay and ELISA.

One final point to be mentioned is the absence of dynamic range for a specific application of the biosensor assay in this paper. In the previous literature reported by Yu and Irudayaraj (2007b), a series of GNRs molecular probes was fabricated and the dynamic response in the range between 10^{-9} M and 10^{-6} M was demonstrated. In our opinion, for the homogeneous assays, it is reasonable to deduce that the dynamic and linear range must probably depend on the concentration, synthesis conditions and the properties of the probe molecules. Once these conditions have been optimized, a suitable dynamic range and an enlarged linear range will be obtained. So, further research has been carried out to give a theoretical model for calculating the linear range of such assays. However, the methodology developed here exhibits a good linear rule in low concentrations and will offer a valuable tool to test the samples with low virus loads which could not be confirmed by routine ELISA.

4. Conclusion

In this work, a homogeneous, label-free plasmonic biosensor has been successfully fabricated using anisotropic gold nanorods. Taking the detection of HBsAg as an example, investigation of the HBsAb-modified GNRs indicates that the physical adsorption and successively blocking lead to a flexible shell enveloping the nanorod, which minimizes the nonspecific adsorption and allows such assays to work in buffer, serum and plasma. A validation experiment was designed based on ELISA and demonstrated that the steric effect would not affect much of the binding affinity of the antigen/antibody pair. The sensor response to HBsAg standard material binding to the probe in Tris buffer was concentration-dependent, with the range from 0.01 IU/mL to 1 IU/mL, with a detection limit of 0.01 IU/mL. Additionally, the homogeneous detection mode offers the possibility of monitoring biological interactions simultaneously and provides a useful means to estimate the kinetics parameters.

Acknowledgements

The authors gratefully acknowledge financial support from the Chinese National 863 Plan (2006AA03Z326) and the National Science Foundation of China (30701002). The authors thank Professor Xiaochun Wu (National Center for Nanoscience and Nanotechnology) and Professor Lin Guo (Beijing University of Aeronautics and Astronautics) for their helpful discussions and scientific advices, and also thank Professor Yiguang Jin and Dr. Miao Li for technology support in characterizations.

References

Anker, J.N., Hall, W.P., Lyandres, O., Shah, N.C., Zhao, J., Van Duyne, R.P., 2008. Nat. Mater. 7, 442–453.
Baselt, D.R., Lee, G.U., Natesan, M., Metzger, S.W., Sheehan, P.E., Colton, R.J., 1998. Biosens. Bioelectron. 13 (7–8), 731–739.
Caswell, K.K., Wilson, J.N., Bunz, U.H.F., Murphy, C.J., 2003. J. Am. Chem. Soc. 125 (46), 13914–13915.
Chang, J.-Y., Wu, H., Chen, H., Ling, Y.-C., Tan, W., 2005. Chem. Commun. 8, 1092–1094.
Chen, C.-D., Cheng, S.-F., Chau, L.-K., Wang, C.R.C., 2007. Biosens. Bioelectron. 22 (6), 926–932.
Demidov, V.V., 2005. Exp. Rev. Mol. Diagn. 4 (3), 267–268.
Foucault, R., Birke, R.L., Lombardi, J.R., 2003. Langmuir 19 (21), 8818–8827.
Gaster, R.S., Hall, D.A., Nielsen, C.H., Osterfeld, S.J., Yu, H., Mach, K.E., Wilson, R.J., Murmann, B., Liao, J.C., Gambhir, S.S., Wang, S.X., 2009. Nat. Med. 15 (11), 1327–1333.
Ghosh, S., Sood, A.K., Kumar, N., 2003. Science 299 (5609), 1042–1044.
Graham, D.L., Ferreira, H., Bernardo, J., Freitas, P.P., Cabral, J.M.S., 2002. J. Appl. Phys. 91 (10), 7786–7788.
Huang, X., El-Sayed, I.H., Qian, W., El-Sayed, M.A., 2007. Nano Lett. 7 (6), 1591–1597.
Huang, H., Huang, S., Liu, X., Zeng, Y., Yu, X., Liao, B., Chen, Y., 2009. Biosens. Bioelectron. 24 (10), 3025–3029.
Huang, H., Liu, X., Hu, T., Chu, P.K., 2010. Biosens. Bioelectron., doi:10.1016/j.bios.2010.02.003.
Hutter, E., Fendler, J.H., 2004. Adv. Mater. 16 (19), 1685–1706.
Jain, K.K., 2004. Exp. Rev. Mol. Diagn. 358 (1–2), 37–54.
Kalyanasundaram, K., Thomas, J.K., 1976. J. Phys. Chem. 80 (13), 1462–1473.
Kelly, K.L., Coronado, E., Zhao, L.L., Schatz, G.C., 2003. J. Phys. Chem. B 107 (3), 668–677.
Li, G., Joshi, V., White, R.L., Wang, S.X., Kemp, J.T., Webb, C., Davis, R.W., Sun, S., 2003. J. Appl. Phys. 93 (10), 7557–7559.
Li, G., Sun, S., Wilson, R.J., White, R.L., Pourmand, N., Wang, S.X., 2006. Sens. Actuators A Phys. 126 (1), 98–106.
Liu, X., Dai, Q., Austin, L., Coutts, J., Knowles, G., Zou, J., Chen, H., Huo, Q., 2008. J. Am. Chem. Soc. 2130 (9), 2780–2782.
Marinakos, S.M., Chen, S., Chilkoti, A., 2007. Anal. Chem. 79 (14), 5278–5283.
Mayer, K.M., Lee, S., Liao, H., Rostro, B.C., Fuentes, A., Scully, P.T., Nehl, C.L., Hafner, J.H., 2008. ACS Nano 2 (4), 687–692.
Millen, R.L., Kawaguchi, T., Granger, M.C., Porter, M.D., 2005. Anal. Chem. 77 (20), 6581–6587.
Murphy, C.J., Sau, T.K., Gole, A.M., Orendorff, C.J., Gao, J., Gou, L., Hunyadi, S.E., Li, T., 2005. J. Phys. Chem. 109 (29), 13857–13870.
Nusz, G.J., Curry, A.C., Marinakos, S.M., Wax, A., Chilkoti, A., 2009. ACS Nano 3 (4), 795–806.
Osterfeld, S.J., Yu, H., Gaster, R.S., Caramuta, S., Xu, L., Han, S.-J., Hall, D.A., Wilson, R.J., Sun, S., White, R.L., Davis, R.W., Pourmand, N., Wang, S.X., 2008. Proc. Natl. Acad. Sci. U.S.A. 105 (52), 20637–20640.

Pérez-Juste, J., Pastoriza-Santos, I., Liz-Marzán, L.M., Mulvaney, P., 2005. Coord. Chem. Rev. 249, 1870–1901.
Pramod, P., Joseph, S.T.S., Thomas, K.G., 2007. J. Am. Chem. Soc. 129 (21), 6712–6713.
Sau, T.K., Murphy, C.J., 2004. Langmuir 20 (15), 6414–6420.
Shingyoji, M., Gerion, D., Pinkel, D., Gray, J.W., Chen, F., 2005. Talanta 67 (3), 472–478.
Wang, C., Irudayaraj, J., 2008. Small 4 (12), 2204–2208.
Wang, C., Irudayaraj, J., 2009. Small 6 (2), 283–289.
Wang, L., Chen, W., Xu, D., Shim, B.S., Zhu, Y., Sun, F., Liu, L., Peng, C., Jin, Z., Xu, C., Kotov, N.A., 2009. Nano Lett. 9 (12), 4147–4152.
Weissleder, R., 2001. Nat. Biotechnol. 19 (4), 316–317.
Xia, X., Xu, Y., Zhao, X., Li, Q., 2009. Clin. Chem. 55 (1), 179–182.
Yu, C., Irudayaraj, J., 2007a. Anal. Chem. 79 (2), 572–579.
Yu, C., Irudayaraj, J., 2007b. Biophys. J. 93 (10), 3684–3692.
Yu, C., Varghese, L., Irudayaraj, J., 2007. Langmuir 23 (17), 9114–9119.
Zheng, G., Patolsky, F., Cui, Y., Wang, W.U., Lieber, C.M., 2005. Nat. Biotechnol. 23, 1294–1301.